

## RESEARCH

# Diagnostic accuracy of proximal enamel subsurface demineralization and its relationship with calcium loss and lesion depth

E Önem<sup>1</sup>, BG Baksi<sup>\*1</sup>, BH Şen<sup>2</sup>, Ö Söğüt<sup>3</sup> and A Mert<sup>4</sup>

<sup>1</sup>Ege University, School of Dentistry, Department of Oral Diagnosis and Radiology, Izmir, Turkey; <sup>2</sup>Ege University, School of Dentistry, Department of Restorative Dentistry and Endodontology, Izmir, Turkey; <sup>3</sup>Ege University, Faculty of Pharmacy, Department of Analytical Chemistry, Izmir, Turkey; <sup>4</sup>Ege University, Faculty of Science, Department of Statistics, Izmir, Turkey

**Objective:** The aim of this study was to determine the relationship between the amount of calcium loss, lesion depth, and the accuracy of storage phosphor plate (SPP) and film radiographs for the detection of artificial proximal demineralization.

**Methods:** Standard enamel windows of extracted premolars were exposed to a demineralizing solution for 60 h, 80 h, 100 h and 120 h. Solutions were analysed for calcium concentration by atomic absorption spectrometer and the lesion depths were calculated by a specific formula. All teeth were radiographed with SPPs and F-speed films before and after acid application. Images were evaluated by five observers. Stereomicroscopic and scanning electron microscopic (SEM) observations were carried out to visualize enamel surfaces after acid exposure. Receiver operating characteristic analysis was used for diagnostic accuracy ( $A_z$ ).  $A_z$ s were compared with factorial analysis of variance and *t*-tests. The relationship between  $A_z$ s and lesion depths was determined with Pearson's correlation test.

**Results:** Strong positive correlation was found between  $A_z$ s of both radiographic methods and lesion depths. No difference was found between the  $A_z$ s of two radiographic systems for any of the demineralization durations ( $p > 0.05$ ). Pair-wise comparisons revealed no significant difference in  $A_z$ s of SPPs ( $p > 0.05$ ), while significant differences were obtained for the  $A_z$ s of films for different demineralization periods ( $p < 0.05$ ). Stereomicroscopic and SEM observations confirmed demineralizations from superficial to deeper layers of enamel.

**Conclusion:** Subsurface enamel demineralization was not accurately detectable with either storage phosphor plates or F-speed films. The amount of calcium loss and the depth of demineralization have a strong relationship with diagnostic accuracy with a significant effect particularly on F-speed films.

*Dentomaxillofacial Radiology* (2012) 41, 285–293. doi: 10.1259/dmfr/55879293

**Keywords:** enamel demineralization; radiography; film; storage phosphor plate; calcium loss

## Introduction

Caries lesions should be detected as early as possible, even before the non-cavitated stage of lesion formation, in order to accomplish successful preventative intervention.<sup>1,2</sup> The performance of different radiographic methods for the early detection of approximal caries has been tested in numerous studies.<sup>3,4</sup> In addition,

the accuracy of alternative methods such as image analysis and/or processing techniques has been tested in an attempt to overcome some of the insufficiencies of radiography for the early detection of enamel caries.<sup>5,6</sup> In addition to the radiographic methods, the detection capacity of some novel diagnostic techniques such as fibre optic transillumination and quantitative light or laser-induced fluorescence has been investigated.<sup>7</sup> However, most of these studies reported the accuracy of the method demonstrating one of the preferred reporting metrics, namely sensitivity, specificity, area under the receiver operating characteristic (ROC) curve

\*Correspondence to: Dr B. Güniz Baksi, Ege Üniversitesi, Dishekimligi Fakültesi, Oral Diagnoz and Rad AD, Bornova, 35100, Izmir, Turkey.  
E-mail: bgunb@yahoo.com

Received 5 January 2011; revised 22 February 2011; accepted 3 March 2011

and the correlation with the truth (true state of disease established using a gold standard).<sup>7</sup>

Radiographic detection of dental caries is primarily based on the fact that as the caries process proceeds, the mineral content of enamel and dentine decreases with a resultant decrease in the attenuation of the X-ray beam passing through the teeth.<sup>8</sup> The available information in regard to the relationship between the amount of mineral loss and accuracy of radiographic detection is rare and inconsistent. Wenzel<sup>9</sup> claimed that lesions confined to enamel may not be evident radiographically until approximately 30–40% enamel demineralization has occurred. On the other hand, Yang and Dutra<sup>10</sup> stated that 40–60% of tooth decalcification was required for a lesion to be seen radiographically. In their early study, Halse *et al*<sup>11</sup> stated that original radiographs were comparable with subtraction images for the lesions presenting 5–10% mineral loss. The performance of different radiographic methods for the detection of enamel subsurface demineralization was compared previously by many researchers.<sup>12–15</sup> However, there is no study demonstrating the performance of different intraoral radiographic methods for the detection of artificial enamel demineralization in correlation with the amount of calcium loss and lesion depth. Therefore, the aim of this study was to determine the relationship between the amount of calcium loss, lesion depth and the diagnostic accuracy of the Digora<sup>®</sup> Optime (Soredex Corporation, Tuusula, Finland) image plate system and F-speed film (Carestream Kodak, Rochester, NY) for the detection of approximal enamel subsurface demineralization.

## Materials and methods

### *Tooth preparation and demineralization*

60 extracted human permanent premolars without fillings and with intact proximal surfaces were used in the study. After the approximal areas of test teeth were visually inspected to exclude any white or brown spot lesions, they were radiographed to confirm and to ensure that no approximal radiolucency could be seen on the images in order to prevent any diagnostic error.

The teeth were mounted in blocks of silicone with one test tooth and two non-test teeth in each block (Figure 1a). The non-test teeth at either end created natural contact points. Before the teeth were embedded in silicone, both the crowns and roots of all teeth were covered with acid-resistant varnish (Diamond Strength; Sally Hansen, Morris Plains, NJ) except for a circular window about 1.4 mm in diameter (area = 1.54 mm<sup>2</sup>) on one of the proximal surfaces. In order to produce standard circular windows for acid application, standard circular rubbers were prepared with a rubber dam punch and applied to the proximal surfaces of the test teeth before varnish application (Figure 1b). After the varnish was dried, the rubber was removed from the surface.

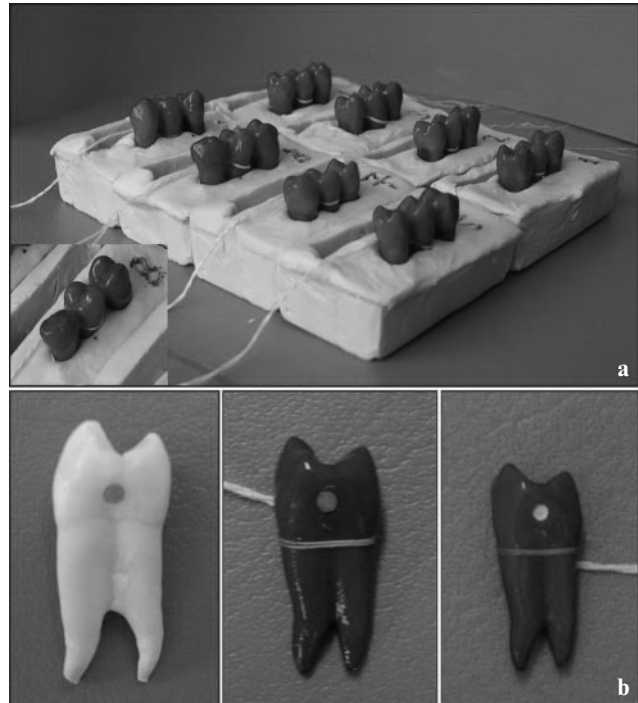


**Figure 1** (a) Test teeth in contact with non-test teeth on two sides mounted in silicone blocks. (b) Test tooth covered with nail varnish other than the area of acid application (white area) on proximal surface

The images of teeth with intact approximal areas obtained prior to any acid application (demineralization) were used as controls. This group of images was named as “0 h group”.

Acetic acid buffer with 0.34 M sodium acetate (pH 4) was used for inducing enamel subsurface demineralization.<sup>16</sup> Pilot studies were carried out with five permanent premolar teeth to decide the duration of acid application in order to create lesions confined only to enamel. After the images of five teeth were obtained with both systems, they were evaluated by two radiologists and one specialist in restorative dentistry with clinical experience of at least 20 years. It was observed that acid durations longer than 120 h produced large lesions easily detectable with any imaging modality. Therefore, longer durations were not used in the study (Figure 2).

Each experimental tooth was de-mounted from its individual block and immersed in 20 ml of acetic acid buffer solution (pH 4.0) at 37°C in individual bottles ( $n = 20$ ). The immersion periods were 60 h, 80 h, 100 h and 120 h. By the end of each immersion period, each tooth was removed from its bottle and replaced in its own block. Then, each block was radiographed with two different imaging modalities as explained below. Following radiography, the teeth were immersed in fresh acidic solutions in new bottles for an additional 20 h. The prior solution in each previous bottle was analysed for calcium amount by an atomic absorption spectrometer (AAS) (wavelength 422.7 nm, slit 0.5 nm) (Spectra AA 10 plus, Varian,

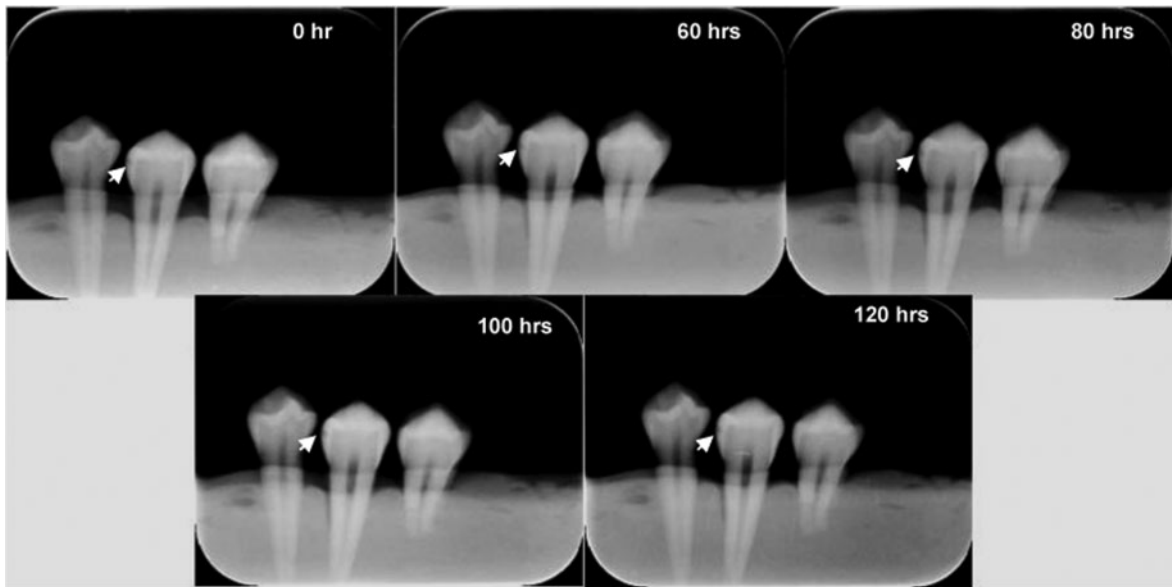


**Figure 2** Images obtained before demineralization (0h) and after four demineralization durations

Mulgrave, VIC, Australia). To prevent the interaction of magnesium and phosphate ions, 50 000 mg l<sup>-1</sup> of lantana chlorine (LaCl<sub>2</sub>) was added in each sample and demineralizing solution.

After measurement of calcium amount by AAS, it was converted into the lesion depth through a specific formula.<sup>17,18</sup> Enamel has a density of 2.95 g ml<sup>-1</sup><sup>19</sup> and calcium concentration in enamel is 37%.<sup>20,21</sup> Enamel volume was calculated using the amount of calcium released into the solution and the density of enamel. It was then divided by the area of the exposed window (1.54 mm<sup>2</sup>) to determine the lesion depth.<sup>22,23</sup>

#### *Radiographic method*

Standardized exposures of all specimens were first done before any acid treatment and on the last day of each demineralization period. All teeth were radiographed with two different imaging modalities—Digora Optime storage phosphor plate (SPP) system (Soredex Corp., Tuusula, Finland) and F-speed film (Carestream Kodak, Rochester, NY). F-speed films and SPPs were exposed with a dental X-ray unit operating at 60 kVp, 7 mA and 1.5 mm Al equivalent filtration using bite-wing projection geometry at a focus–receptor distance of 25 cm (Figure 3). With regards to the examinations with film and image plates, vinyl polysiloxane putty was adapted to the positioning device, and while the putty was still soft, both the detector and silicone block were pressed into it. Once hardened, the putty allowed quick realignment of the specimen and the detector. This assembly was made for each block (Figure 3). A 20 mm thick soft-tissue equivalent material was placed close to the blocks and facing the X-ray tube. Films and SPPs were exposed for 0.20 s and 0.12 s, respectively, to subjectively generate an optimal density for caries detection.<sup>24–27</sup> After the plates were scanned, the resulting

images were exported as eight-bit TIFF files for subsequent display in a random order. Films were developed using an AP-200 (PLH Medical Ltd, Watford, UK) automatic processor with fresh solutions and with a processing time of 6 min at 23.5 °C. The processed radiographs were mounted in non-transparent frames.

#### *Image evaluation*

Three radiologists and two specialists in restorative dentistry with a mean age of 39.8 years (range 31–59 years) and mean clinical experience of 18.0 years (range 8–40 years) acted as evaluators and independently rated the presence/absence of proximal demineralization using a five-graded scale:

1. definitely present
2. probably present
3. unsure
4. probably absent
5. definitely absent.

Observers were instructed to assess only proximal surfaces coronal to the cemento-enamel junction. Any sign of demineralization was to be considered enamel subsurface demineralization, regardless of size and degree of penetration into enamel.

5 independent observers assessed a total of 200 digital and film radiographs (2 systems × 20 teeth × 5 time periods). To simulate a clinical situation, observers rated the one approximal surface of each test tooth and the approximal surface of the adjacent tooth for the presence/absence of demineralization. A total of 400 surfaces were rated by each observer. The images were displayed to observers at full size, 1:1 on a 15.4 inch high resolution (WXGA) colour liquid crystal monitor with a resolution of 1024 × 768 pixels and 256 grey

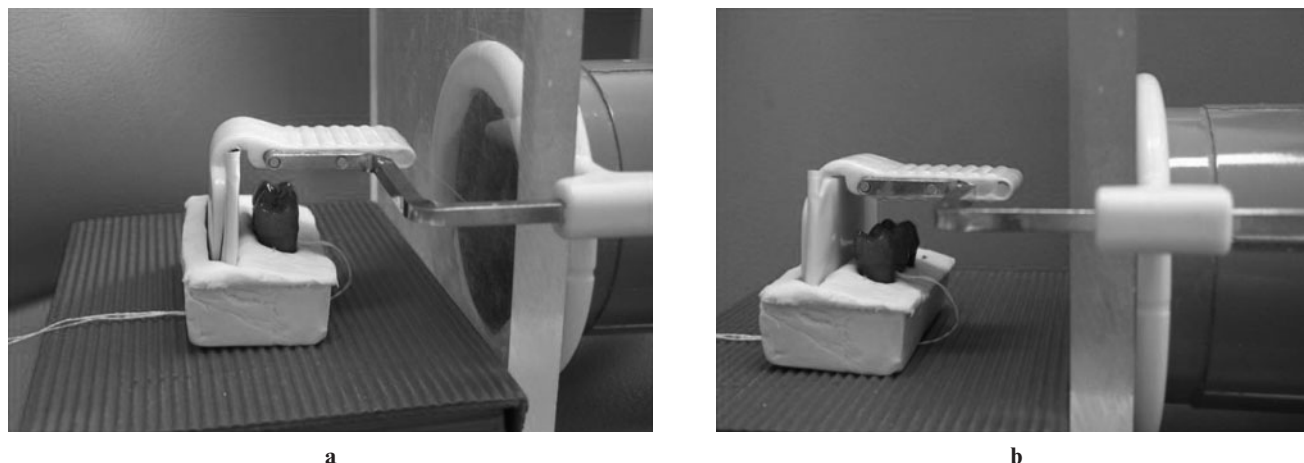


**Figure 3** Picture demonstrating the bite-wing projection geometry during exposures

levels (HP Pavillion DV6000, Santa Clara, CA). Observation conditions were optimized through the use of the same computer monitor when the images were displayed and the viewing distance was kept constant to about 50 cm for all observers and the lights were subdued during observations. For each image modality, all images were presented in a randomized order. A moderator presented each image for viewing and maintained proper random sequence order. 4 separate viewing sessions (50 films or images per session) were held at intervals of at least 1 week to minimize viewer fatigue and to decrease the chance of recalling previous decisions on similar images. The observers were not given the option to perform any image enhancements to avoid the production of a variety of different digital images. The film radiographs were assessed using a light box and at 2 $\times$  magnification (RINN, Dentsply, Elgin, IL). No time limit was set for the viewing procedure.

#### *Microscopic evaluations*

Two extra premolar teeth for each time period were prepared and demineralized in the above-mentioned manner for stereomicroscopic (Leica S8APO, Heerbrugg, Switzerland) and scanning electron microscopic (SEM) (JSM-5200, JEOL, Tokyo, Japan) observations to visualize enamel surfaces after acid exposure.

#### *Data analysis*

The diagnostic accuracy on images obtained after different periods of demineralization was expressed as the area under the ROC curves ( $A_z$ ). ROC analysis was carried out for each observer, each demineralization period and each image modality and then ROC areas for all five observers were averaged to obtain a mean value. GraphPad InStat (GraphPad Software, Inc., La Jolla, CA) was used for statistical analysis. Comparison of mean  $A_z$ s was done with factorial analysis of variance (ANOVA) as the imaging system, demineralization period and observers were the factors. Pair-wise

comparisons were performed using post hoc *t*-tests ( $p = 0.05$ ). Kappa ( $\kappa$ ) was used to measure the inter-observer agreement. Pearson's correlation test was used to reveal any possible relationship between  $A_z$  values and lesion depths ( $p = 0.05$ ).

#### **Results**

The mean amount of calcium loss  $\pm$  standard deviation (SD) for four different demineralization durations (60 h, 80 h, 100 h and 120 h) were  $26.38 \pm 14.18 \mu\text{g ml}^{-1}$ ,  $30.69 \pm 18.68 \mu\text{g ml}^{-1}$ ,  $35.56 \pm 18.83 \mu\text{g ml}^{-1}$  and  $50.08 \pm 23.18 \mu\text{g ml}^{-1}$ , respectively (Figure 4). Calcium loss was slow and showed an almost linear increase with increasing acid duration. The mean lesion depths  $\pm$  SD for demineralization periods of 60 h, 80 h, 100 h and 120 h were  $15.71 \pm 8.44 \mu\text{m}$ ,  $18.27 \pm 10.56 \mu\text{m}$ ,  $21.12 \pm 11.41 \mu\text{m}$  and  $29.76 \pm 16.05 \mu\text{m}$ , respectively (Figure 4). A significant difference in lesion depths was observed between 60 h vs 120 h ( $p < 0.01$ ) and 80 h vs 120 h of demineralization ( $p < 0.05$ ).

The mean  $A_z$  values for 60 h, 80 h, 100 h and 120 h of demineralization were 0.592, 0.603, 0.604 and 0.717, respectively, for SPPs and 0.538, 0.562, 0.727 and 0.797, respectively, for F-speed films (Table 1). Pair-wise comparisons revealed that the  $A_z$ s of SPPs were not significantly different for any demineralization period ( $p > 0.05$ ). On the contrary, significant differences were obtained for the  $A_z$ s of films for different periods of demineralization ( $p < 0.05$ ). The difference was significant between 60 h vs 100 h ( $p < 0.05$ ), 60 h vs 120 h ( $p < 0.05$ ), 80 h vs 100 h ( $p < 0.05$ ) and 80 h vs 120 h ( $p < 0.05$ ). No difference was found between the corresponding  $A_z$ s of two imaging systems for any of the demineralization periods ( $p > 0.05$ ). The mean standard deviations of the  $A_z$  values were lower for the film images than for storage phosphor plates (Table 1).

For both systems, the agreement was fair for 60 h (range 0.28–0.37 h), 80 h (range 0.31–0.39 h) and 100 h

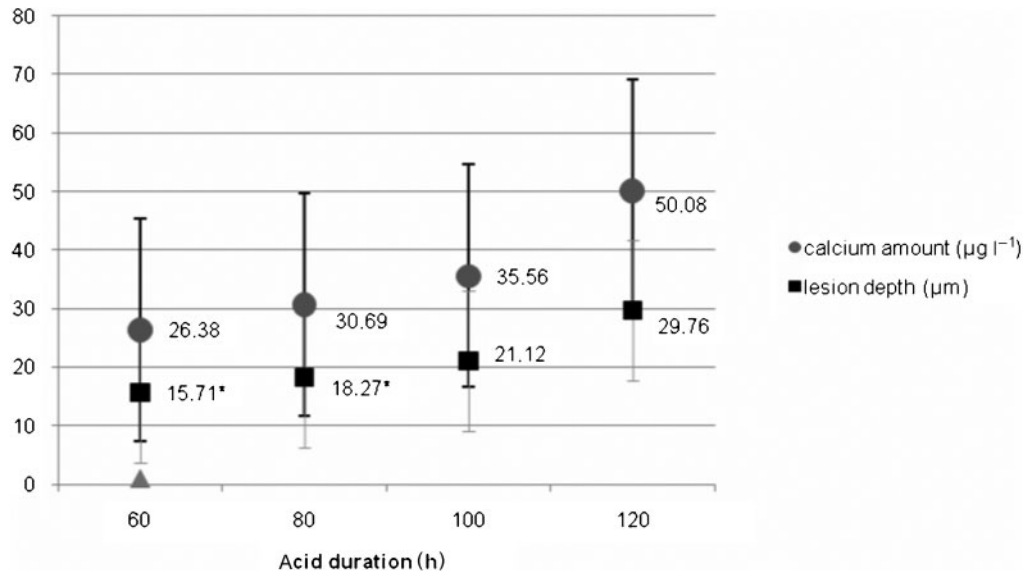


**Figure 4** Mean calcium amounts ( $\mu\text{g l}^{-1}$ )  $\pm$  standard deviation (SD) and calculated lesion depths ( $\mu\text{m}$ )  $\pm$  SD for each demineralization duration. \* Indicates significance with depth obtained after 120 h of demineralization

(range 0.33–0.40 h) of demineralization and substantial (range 0.44–0.58 h) for 120 h demineralization.

Strong positive correlation was found between  $A_z$  values of both film and SPP images and lesion depths. While this correlation was linear for SPPs ( $r = 0.9579$ ;  $p = 0.042$ ), it was non-linear for films ( $r = 0.9193$ ;  $p = 0.08$ ). Further analysis showed that the relationship between film and lesion depth fit to a geometric model ( $y = x^{-0.496}$ ;  $r = 0.97$ ,  $p = 0.03$ ).

Stereomicroscopic and SEM observations revealed lesions from superficial to deeper layers of enamel (Figures 5 and 6). Acid application affected the exposed enamel partially or totally in different samples (Figures 5 and 6). After 120 h of demineralization, all proximal areas showed clearly visible white spots after air drying. This finding was confirmed by light microscopic analysis (Figure 5). In some of the samples, based on SEM images, erosions could be observed only at the borders of the circular window after demineralization (Figure 6d).

## Discussion

It has been clearly stated in a radiology book<sup>9</sup> and a review article<sup>10</sup> that enamel proximal caries lesions are poorly detected by radiography since demineralization must occur in excess of 30% for radiographic detection

to be possible. However, in both references, this information was not cited to any scientific study and remains vague. Although there was a single study that might be related to the subject, the authors did not actually measure the mineral loss in this study.<sup>11</sup>

In our present study, atomic absorption spectroscopy was used for measurements of calcium levels after various demineralization durations. The measured calcium amounts were then used to calculate the mean lesion depth from the surface. Although the determination of lesion depth by use of calcium loss is an indirect method, it was shown to be a reliable method for analysing the progression of etch depth related to successive acid exposures on the same enamel surfaces.<sup>28</sup> It was also demonstrated that this method was comparable to the direct methods such as white light interferometry and light profilometry.<sup>28</sup> If one considers the definition of caries as a demineralization/remineralization imbalance leading to net mineral loss, mineral loss should be the parameter of a carious lesion that should be measured. However, considering the direction of progression and the relationship between the defence reaction of the tooth and depth of progression, depth of mineral loss may be as relevant as volume of mineral loss.<sup>29</sup>

There are numerous studies in dental literature comparing the diagnostic accuracy of digital and conventional radiography for the detection of either artificial or natural proximal caries. Most of these studies have

**Table 1** Accuracy  $\pm$  standard deviation obtained with F-speed films and storage phosphor plate (SPP) images after 60 h, 80 h, 100 h and 120 h of acid demineralization

	60 h	80 h	100 h	120 h
SPP	0.59 $\pm$ 0.11	0.60 $\pm$ 0.05	0.60 $\pm$ 0.05	0.72 $\pm$ 0.05
Film	0.53 $\pm$ 0.09 <sup>a,b</sup>	0.56 $\pm$ 0.05 <sup>a,b</sup>	0.73 $\pm$ 0.04	0.79 $\pm$ 0.04

<sup>a</sup> Indicates significance with 100 h of demineralization.

<sup>b</sup> Indicates significance with 120 h of demineralization.

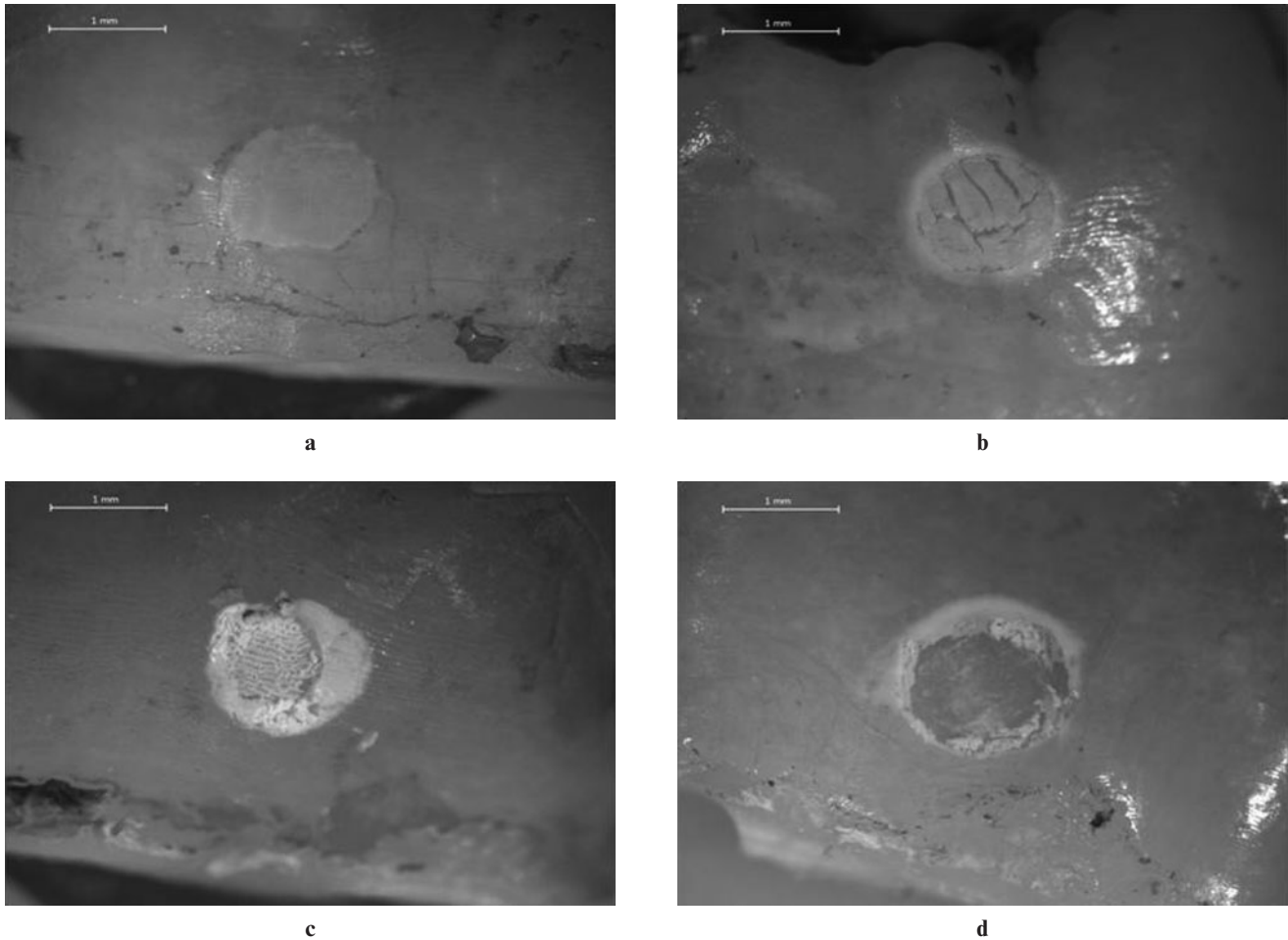


**Figure 5** Stereomicroscopic images obtained after 60 h (a), 80 h (b), 100 h (c) and 120 h (d) of demineralization (magnification  $\times 20$ )

included evaluation of lesions extending from enamel to dentine by mainly focusing on lesion detection (present or absent) using various imaging methods.<sup>6,30–32</sup> However, the relationship between the depth of enamel lesions and visual assessment of observers was investigated in few studies.<sup>33,34</sup> The capacity of several radiographic methods for the detection of different degrees of enamel demineralization was investigated as well. Nevertheless, they either used subtraction radiography to evaluate the resultant images for detection of enamel demineralization<sup>12,14</sup> or compared the performance of advanced diagnostic methods such as digital imaging fibre-optic transillumination or polarization-sensitive optical coherence tomography for the evaluation of the relationship between lesion depth and diagnostic accuracy.<sup>35,36</sup> Owing to the difficulties in combining quantitative methods for mineral determination and methods for obtaining the radiographic image of the same teeth for visual evaluation, no study can be found correlating the amount of calcium loss, lesion depth and the diagnostic accuracy of digital and conventional radiography for the detection of artificial enamel demineralization. In this context, the present study is the first to demonstrate the relationship among

the amount of calcium loss, depth of demineralization and the diagnostic accuracy of storage phosphor plates and F-speed films.

According to our results, a strong relationship was found between lesion depth and diagnostic accuracy of enamel demineralization on both SPP and film images. This result can already be anticipated because as the demineralization proceeds, the mass difference between the lesion and surrounding sound tissue gets larger, contributing to a higher signal-to-noise ratio and higher image contrast. Although this result is in accordance with the results of Castro *et al*,<sup>33</sup> it is contradictory to the results of Pontual *et al*,<sup>34</sup> who reported no increase in detection with increasing depth of enamel lesions. When the methods of the latter study were closely evaluated, it was observed that they used double the amount of exposure (0.25 s) than the exposure time used in this study for blue Digora SPPs. In order to extrapolate our results to clinical settings, the plates in this study were exposed for 0.12 s as recommended for patient exposure.<sup>37–39</sup> As exposure is increased in the SP systems, the signal-to-noise ratio is also increased and the ability to visualize details is improved.<sup>40</sup> Therefore, the insignificant relationship between the

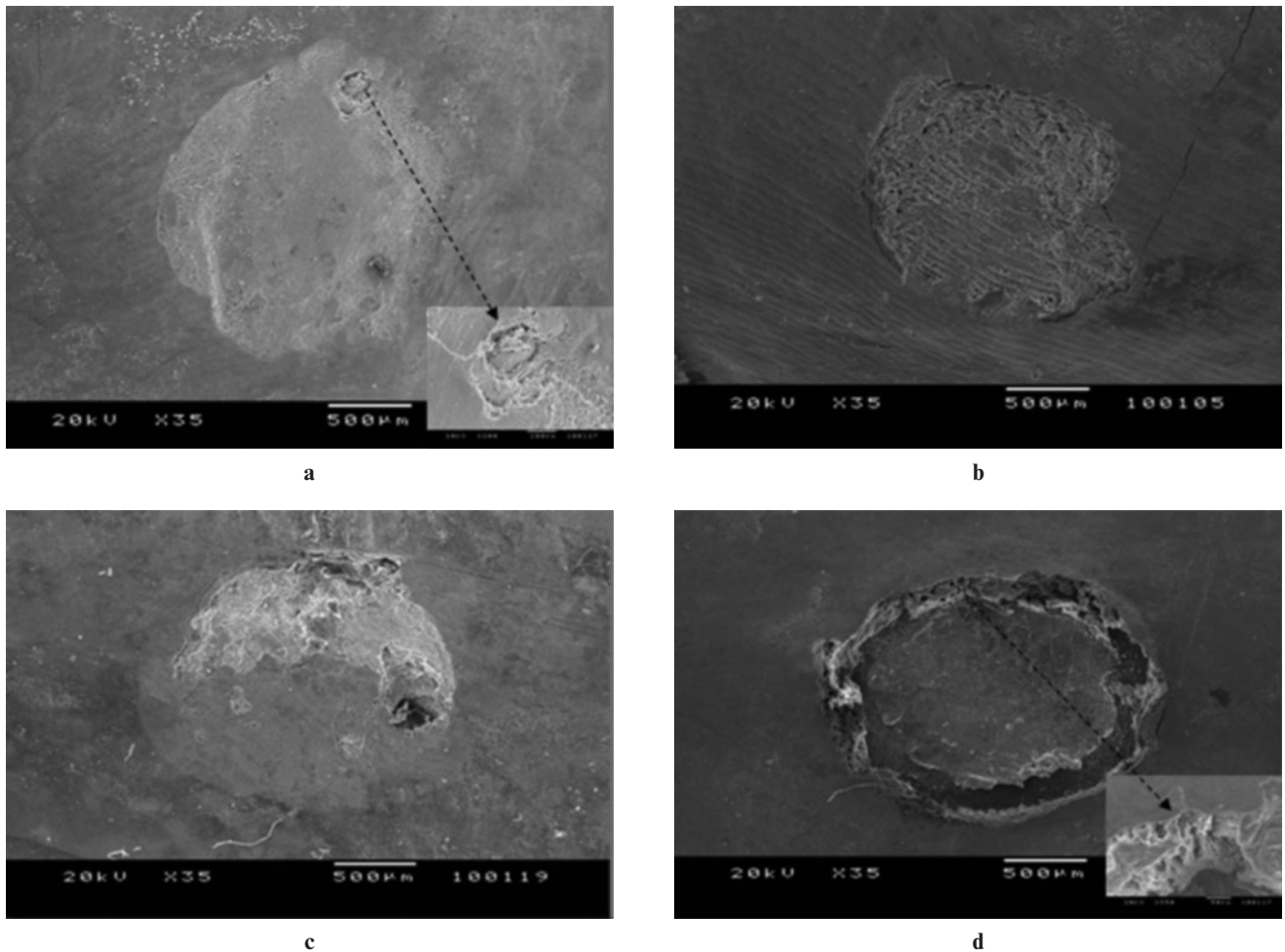


**Figure 6** Scanning electron microscopy images of demineralization areas (a) 60 h, (b) 80 h, (c) 100 h and (d) 120 h (magnification  $\times 35$ ). Inserts in images (a) and (d) show the  $\times 200$  magnification of the areas demonstrated by black arrows

diagnostic accuracy and the depth of enamel caries as reported by Pontual *et al*<sup>34</sup> may be due to the consequent reduction in image noise and increase in image density with increased exposure time.

Diverging results from different studies must be carefully investigated when directly compared, as differences in the experimental design, the lesion type and the number of scoring categories and observers may influence the outcome.<sup>13</sup> For example, different demineralization models may lead to varying caries patterns and progression rates. In addition, artificial lesions created with burs may differ from chemically created enamel demineralization.<sup>41–43</sup> Accordingly, another factor for the varying results in relationship between diagnostic accuracy and depth of enamel demineralization may be the performance of the observers in accordance with the lesion type. It has been clearly demonstrated that lesion type has an influence on radiographic estimation of caries.<sup>44</sup> In addition, the depth of the lesion significantly affects the performance of the observers.<sup>3</sup> In the present study, the highest amount of lesion depth with an average of

approximately  $30\ \mu\text{m}$  was calculated from the amount of calcium loss after 120 h of acid demineralization. In addition, SEM and stereomicroscopic observations confirmed that enamel demineralization was confined only to superficial layers of enamel tissue.<sup>45,46</sup>

Incipient enamel lesions deliberately selected to be more difficult for visual perception may be a contributing factor for the significant relationship between diagnostic accuracy and depth of enamel demineralization found in the present study. The increase in agreement with increasing lesion depths for both systems has further supported this assumption.

Diagnostic accuracy for relatively short demineralization durations (60 h and 80 h) was close to guesswork for both diagnostic systems. This finding is in agreement with many previous studies.<sup>6,34,47</sup> The diagnostic accuracy of the 120 h lesions (with an average depth of around  $30\ \mu\text{m}$ ) was approximately 0.71 for SPPs and 0.80 for F-speed films. In two consecutive studies by the same group,<sup>15,48</sup> artificial demineralization depths ranged between  $230\ \mu\text{m}$  and  $410\ \mu\text{m}$  while corresponding accuracy (0.89) for SPPs was higher than the accuracy

obtained in the present study. Higher diagnostic accuracy for lesions approximately 8–14 times deeper from the tooth surface towards the pulp can be anticipated; nonetheless, any relationship between lesion depth and diagnostic accuracy was not investigated in either of the studies. On the other hand, Schmidlin *et al*<sup>13</sup> produced both 0.1 mm deep chemical enamel demineralization and artificial enamel lesions with burs having sequentially increasing depths (0.1–0.5 mm). While a significant relationship was reported between lesion depth and sensitivity for artificial bur lesions, it was shown that 0.1 mm deep chemically- created demineralization was not detectable by visual radiographic examination (sensitivity = 0). Visual assessment of chemically created demineralization on SPP images in the former study was made using a dichotomous scale — a simple two-point scale (no lesion = 1, lesion = 2). It is well known that the use of continuous scoring (five-graded scale) increases discrimination, which may explain the difference between the results of Schmidlin *et al*<sup>13</sup> and the present study with regards to the diagnostic accuracy of enamel demineralization.

The results showed no significant difference between the diagnostic accuracy of the two systems. However, F-speed films showed a slightly higher level of diagnostic accuracy than the digital images. Although none of the systems performed significantly better or worse than the other for any particular depth of demineralization, the depth of enamel lesion seems to influence the accuracy of the films more than it did the accuracy of SPPs. A significant difference was found in detection accuracy of films between lower and relatively higher lesion

depths. The comparable accuracy of SPP and film images for detection of proximal demineralization was in accordance with many previous studies.<sup>3,49</sup> On the other hand, the significant increase in the accuracy of films with increasing lesion depths may be due to its higher spatial and contrast resolution characteristics since detection of enamel lesions is strongly influenced by resolution parameters.<sup>49</sup>

If the detection methods are accurate and objective enough, the disease can be followed over time and the rate of progress or reversal can be measured.<sup>50</sup> If an enamel lesion, as detected by the radiograph, is not beyond the dentino-enamel junction, it can be arrested or reversed by remineralization.<sup>46,51</sup> Therefore, early detection of demineralization is extremely important.<sup>51</sup> However, it should be noted that the choice of imaging system/receptor is only one of the many factors affecting the relationship between lesion depth and diagnostic accuracy of enamel demineralization.

A strong relationship was observed between the amount of calcium loss, lesion depth and detectability of artificial enamel demineralization on SPP and film images. However, the low levels of accuracy along with fair agreement for the lower demineralization durations (60 h, 80 h and 100 h) reflect the difficulty examiners had in deciding whether there had been demineralization or not with both of the image receptors used in this study. Therefore, it is possible to conclude that subsurface enamel demineralization was not accurately detectable with either SPPs or F-speed films and depth of enamel demineralization had a significant effect, particularly on the diagnostic accuracy of F-speed films.

## References

- Pitts NB. Clinical diagnosis of dental caries: a European perspective. *J Dent Educ* 2001; **65**: 972–978.
- Nyvad B. Diagnosis versus detection of caries. *Caries Res* 2004; **38**: 192–198.
- Syriopoulos K, Sanderink GC, Velders XL, van der Stelt PF. Radiographic detection of approximal caries: a comparison of dental films and digital imaging systems. *Dentomaxillofac Radiol* 2000; **29**: 312–318.
- Alkurt MT, Peker I, Bala O, Altunkaynak B. In vitro comparison of four different dental X-ray films and direct digital radiography for proximal caries detection. *Oper Dent* 2007; **32**: 504–509.
- Møystad A, Svanaes DB, van der Stelt PF, Grøndahl HG, Wenzel A, van Ginkel FC, *et al*. Comparison of standard and task-specific enhancement of Digora storage phosphor images for approximal caries diagnosis. *Dentomaxillofac Radiol* 2003; **32**: 390–396.
- Li G, Sanderink GC, Berkhout WE, Syriopoulos K, van der Stelt PF. Detection of proximal caries in vitro using standard and task-specific enhanced images from a storage phosphor plate system. *Caries Res* 2007; **41**: 231–234.
- Pretty IA. Caries detection and diagnosis: novel technologies. *J Dent* 2006; **34**: 727–739.
- Dove SB. Radiographic diagnosis of dental caries. *J Dent Educ* 2001; **65**: 985–990.
- Wenzel A. Dental Caries. In: White SC, Pharoah MJ, eds. *Oral radiology: principles and interpretation*. UK, PA: Mosby Elsevier; 2008. pp. 270–281.
- Yang J, Dutra V. Utility of radiology, laser fluorescence, and transillumination. *Dent Clin North Am* 2005; **49**: 739–752, vi.
- Halse A, Espelid I, Tveit AB, White SC. Detection of mineral loss in approximal enamel by subtraction radiography. *Oral Surg Oral Med Oral Pathol* 1994; **77**: 177–182.
- Eberhard J, Hartman B, Lenhard M, Mayer T, Kocher T, Eickholz P. Digital subtraction radiography for monitoring dental demineralization. An in vitro study. *Caries Res* 2000; **34**: 219–224.
- Schmidlin PR, Tepper SA, Scriba H, Lutz F. In vitro assessment of incipient approximal carious lesions using computer-assisted densitometric image analysis. *J Dent* 2002; **30**: 305–311.
- Haiter-Neto F, Ferreira RI, Tabchoury CP, Bóscolo FN. Linear and logarithmic subtraction for detecting enamel subsurface demineralization. *Dentomaxillofac Radiol* 2005; **34**: 133–139.
- Ferreira RI, Haiter-Neto F, Tabchoury CP, de Paiva GA, Bóscolo FN. Assessment of enamel demineralization using conventional, digital, and digitized radiography. *Braz Oral Res* 2006; **20**: 114–119.
- Tezel H, Ertaş OS, Ozata F, Dalgar H, Korkut ZO. Effect of bleaching agents on calcium loss from the enamel surface. *Quintessence Int* 2007; **38**: 339–347.
- ten Cate B. *Remineralisation of enamel lesions: a study of the physicochemical mechanism* (thesis). Groningen, 1979.
- Ganss C, Lussi A, Klimek J. Comparison of calcium/phosphorus analysis, longitudinal microradiography and profilometry for the quantitative assessment of erosive demineralisation. *Caries Res* 2005; **39**: 178–184.
- Weidmann SM, Weatherell JA, Stella MH. Variations of enamel density in sections of human teeth. *Arch Oral Biol* 1967; **12**: 85–97.



20. Robinson C, Weatherell JA, Hallsworth AS. Variation in composition of dental enamel within thin ground tooth sections. *Caries Res* 1971; **5**: 44–57.
21. Tanaka M, Ono H, Kadoma Y, Imai Y. Incorporation into human enamel of fluoride slowly released from a sealant in vivo. *J Dent Res* 1987; **66**: 1591–1593.
22. al-Khateeb S, ten Cate JM, Angmar-Månsson B, de Josselin de Jong E, Sundström G, Exterkate RA, et al. Quantification of formation and remineralization of artificial enamel lesions with a new portable fluorescence device. *Adv Dent Res* 1997; **11**: 502–506.
23. Sá Roriz Fonteles C, Zero DT, Moss ME, Fu J. Fluoride concentrations in enamel and dentin of primary teeth after pre- and postnatal fluoride exposure. *Caries Res* 2005; **39**: 505–508.
24. Borg E, Gröndahl HG. On the dynamic range of different X-ray photon detectors in intra-oral radiography. A comparison of image quality in film, charge-coupled device and storage phosphor systems. *Dentomaxillofac Radiol* 1996; **25**: 82–88.
25. Kitagawa H, Farman AG, Scheetz JP, Brown WP, Lewis J, Benefiel M, et al. Comparison of three intra-oral storage phosphor systems using subjective image quality. *Dentomaxillofac Radiol* 2000; **29**: 272–276.
26. Kaeppler G, Dietz K, Herz K, Reinert S. Factors influencing the absorbed dose in intraoral radiography. *Dentomaxillofac Radiol* 2007; **36**: 506–513.
27. Sakurai T, Kawamata R, Kozai Y, Kaku Y, Nakamura K, Saito M, et al. Relationship between radiation dose reduction and image quality change in photostimulable phosphor luminescence X-ray imaging systems. *Dentomaxillofac Radiol* 2010; **39**: 207–215.
28. Stenhagen KR, Hove LH, Holme B, Taxt-Lamolle S, Tveit AB. Comparing different methods to assess erosive lesion depths and progression in vitro. *Caries Res* 2010; **44**: 555–561.
29. Huysmans MC, Longbottom C. The challenges of validating diagnostic methods and selecting appropriate gold standards. *J Dent Res* 2004; **83**: C48–52.
30. Hintze H, Wenzel A, Frydenberg M. Accuracy of caries detection with four storage phosphor systems and E-speed radiographs. *Dentomaxillofac Radiol* 2002; **31**: 170–175.
31. Rockenbach MI, Veeck EB, da Costa NP. Detection of proximal caries in conventional and digital radiographs: an in vitro study. *Stomatologija* 2008; **10**: 115–120.
32. Crombie K, Parker ME, Nortje CJ, Sanderink GC. Comparing the performance of storage phosphor plate and Insight film images for the detection of proximal caries depth. *SADJ* 2009; **64**: 452–459.
33. Castro VM, Katz JO, Hardman PK, Glaros AG, Spencer P. In vitro comparison of conventional film and direct digital imaging in the detection of approximal caries. *Dentomaxillofac Radiol* 2007; **36**: 138–142.
34. Pontual AA, de Melo D, de Almeida S, Bóscolo F, Haiter Neto F. Comparison of digital systems and conventional dental film for the detection of approximal enamel caries. *Dentomaxillofac Radiol* 2010; **39**: 431–436.
35. Young DA, Featherstone JD. Digital imaging fiber-optic transillumination, F-speed radiographic film and depth of approximal lesions. *J Am Dent Assoc* 2005; **136**: 1682–1687.
36. Jones RS, Darling CL, Featherstone JD, Fried D. Imaging artificial caries on the occlusal surfaces with polarization-sensitive optical coherence tomography. *Caries Res* 2006; **40**: 81–89.
37. Yoshiura K, Kawazu T, Chikui T, Tatsumi M, Tokumori K, Tanaka T, et al. Assessment of image quality in dental radiography, part 2: optimum exposure conditions for detection of small mass changes in 6 intraoral radiography systems. *Oral Surg Oral Med Oral Pathol Oral Radiol Endod* 1999; **87**: 123–129.
38. Berkhout WE, Beuger DA, Sanderink GC, van der Stelt PF. The dynamic range of digital radiographic systems: dose reduction or risk of overexposure? *Dentomaxillofac Radiol* 2004; **33**: 1–5.
39. Bhaskaran V, Qualtrough AJ, Rushton VE, Worthington HV, Horner K. A laboratory comparison of three imaging systems for image quality and radiation exposure characteristics. *Int Endod J* 2005; **38**: 645–652.
40. Chotas HG, Floyd CE Jr, Dobbins JT 3rd, Ravin CE. Digital chest radiography with photostimulable storage phosphors: signal-to-noise ratio as a function of kilovoltage with matched exposure risk. *Radiology* 1993; **186**: 395–398.
41. Pitts NB, Renson CE. Further development of a computer-aided image analysis method of quantifying radiolucencies in approximal enamel. *Caries Research* 1986; **20**: 361–370.
42. Nummikoski PV, Martinez TS, Matteson SR, McDavid WD, Dove SB. Digital subtraction radiography in artificial recurrent caries detection. *Dentomaxillofac Radiol* 1992; **21**: 59–64.
43. Wenzel A, Halse A. Digital subtraction radiography after stannous fluoride treatment for occlusal caries diagnosis. *Oral Surg Oral Med Oral Pathol* 1992; **74**: 824–828.
44. Seneadza V, Koob A, Kaltschmitt J, Staehle HJ, Duwenhoegger J, Eickholz P. Digital enhancement of radiographs for assessment of interproximal dental caries. *Dentomaxillofac Radiol* 2008; **37**: 142–148.
45. Fejerskov O, Thylstrup A. *Pathology in dental caries. Textbook of cariology*. Copenhagen: Munksgaard, 1986.
46. ten Cate JM. Remineralization of deep enamel dentine caries lesions. *Aust Dent J* 2008; **53**: 281–285.
47. Svenson B, Welander U, Anneroth G, Söderfeldt B. Exposure parameters and their effects on diagnostic accuracy. *Oral Surg Oral Med Oral Pathol* 1994; **78**: 544–550.
48. Ferreira RI, Haiter-Neto F, Tabchoury CP, Bóscolo FN. In vitro induction of enamel subsurface demineralization for evaluation of diagnostic imaging methods. *J Appl Oral Sci* 2007; **15**: 392–398.
49. Haak R, Wicht MJ, Noack MJ. Conventional, digital and contrast-enhanced bitewing radiographs in the decision to restore approximal carious lesions. *Caries Res* 2001; **35**: 193–199.
50. Featherstone JD. The continuum of dental caries — evidence for a dynamic disease process. *J Dent Res* 2004; **83**: C39–C42.
51. Featherstone JD. The caries balance: contributing factors and early detection. *J Calif Dent Assoc* 2003; **31**: 129–133.